Environ Monit Assess (2010) 170:231–244
DOI 10.1007/s10661-009-1228-7

Comparison of different semi-empirical algorithms to estimate chlorophyll-a concentration in inland lake water

Hongtao Duan · Ronghua Ma · Jingping Xu · Yuanzhi Zhang · Bai Zhang

Received: 4 January 2009 / Accepted: 29 October 2009 / Published online: 12 November 2009

Abstract Based on in situ water sampling and field spectral measurement from June to September 2004 in Lake Chagan, a comparison of several existing semi-empirical algorithms to determine chlorophyll-a (Chl-a) content was made by applying them to the field spectra and in situ chlorophyll measurements. Results indicated that the first derivative of reflectance was well correlated with Chl-a. The highest correlation between the first derivative and Chl-a was at 680 nm. The two-band model, NIR/red ratio of $R_{710/670}$, was also an effective predictor of Chl-a concentration. Since the two-band ratios model is a special case of the three-band model developed recently, three-band model in Lake Chagan showed a higher resolution. The new algorithm named reverse continuum removal relies on the reflectance peak at 700 nm whose shape and position depend strongly upon chlorophyll concentration: The depth and area of the peak above a baseline showed a linear relationship to Chl-a concentration. All of the algorithms mentioned proved to be of value and can be used to predict Chl-a concentration. Best results were obtained by using the algorithms of the first derivative, which yielded R^2 around 0.74 and RMSE around 6.39 μg/l. The two-band and three-band algorithms were further applied to MERIS when filed spectral were resampled with regard to their center wavelengths. Both algorithms showed an adequate precision, and the differences on the outcome were small with $R^2 = 0.70$ and 0.71.

Keywords Field spectral · Lake Chagan · Continuum removal · Three-band model

H. Duan (✉) · R. Ma
State Key Laboratory of Lake Science and Environment, Nanjing Institute of Geography and Limnology, Chinese Academy of Sciences, Nanjing 210008, China
e-mail: htduan@niglas.ac.cn, htduan@gmail.com

J. Xu
State Key Laboratory of Remote Sensing Science, Jointly Sponsored by the Institute of Remote Sensing Applications of Chinese Academy of Sciences and Beijing Normal University, Beijing 100101, China

Y. Zhang
Institute of Space and Earth Information Science, The Chinese University of Hong Kong, Shatin, NT, Hong Kong

B. Zhang
Northeast Institute of Geography and Agricultural Ecology, Chinese Academy of Sciences, Changchun 130012, China

Introduction

Lakes are valuable water resources and can be used for fishing, transport, agriculture, industry,

recreation, and tourism. To date, water quality conditions for numerous lakes around the world have deteriorated so substantially that they are hardly recoverable by natural means of purification. The most common ecological problem of inland water bodies is anthropogenic eutrophication (Ritchie et al. 1990). Chlorophyll-a (Chl-a) is a main parameter for determining the trophic state, which is one of the major factors affecting water environment and produces visible changes on the water surface (Zhang et al. 2002; Giardino et al. 2001). Since Chl-a exists in all algae groups in marine and freshwater systems, Chl-a concentration is an important indicator for the bio-production of inland water bodies. However, traditional field sampling methods used to estimate Chl-a concentration are time consuming and difficult to make for large regional and global studies.

Remote sensing can provide a suitable means to integrate limnological data collected from traditional in situ measurements (Ritchie et al. 1990), and has the advantages of good spatial and temporal coverage and the possibility of measuring many lakes simultaneously (Koponen et al. 2002). Hyperspectral sensing, expected by many to become a standard technology for measuring chlorophyll concentration in water (Richardson 1996), offers the potential to detect water quality variables such as Chl-a by using narrow spectral channels of less than 10 nm, which could otherwise be masked by broadband satellites such as Landsat TM (Schmidt and Skidmore 2001). As a fundamental research tool for the application of current and future hyperspectral sensing systems, field spectroradiometer is presently commonly used to collect reflectance data (Han 2005).

Several methods for estimating Ch-a concentration with remote sensing are being investigated. These methods, including empirical equations and reflectance model, relate spectral reflectance measurements to the concentrations of Chl-a. Many studies have suggested that estimates of Chl-a concentration based on remote spectroscopic measurements may be possible with spectral band ratios and their combinations (Kokaly 2001). These studies used linear regression to predict Chl-a concentration of lakes water from reflectance spectra. In each study, different wavelengths were found to produce high correlations. However, these algorithms, which were developed for particular water bodies and for particular seasons, cannot be used everywhere and at all times of the year (Kutser et al. 2001). The suggested reasons for this are many such as inaccurate atmospheric correction, variability in the concentrations of constituents in the water, and variations in the materials themselves, sensor limitations, and background information influences (Feng et al. 2005). Thus, many issues remain to be examined in establishing the influence of variable Chl-a concentration on the reflectance spectra and extending Chl-a prediction to independent data sets.

The study reported in this paper is to investigate the potential of semi-empirical algorithms for monitoring Chl-a concentration in Lake Chagan. The algorithms chosen from the literature had to perform well in other studies. A new approach named reverse continuum removal was also developed to isolate the peak around 700 nm, and the peak depth and area were used to link the reflectance changes with Chl-a concentration and evaluate the potential of remote-sensing data for inversion.

Study area description

Lake Chagan, located in the northwest of Jilin province, Northeast China (see Fig. 1), is one of the ten largest fresh-water lakes in China. It has a mean surface area of 372 km^2, a mean depth of 2.52 m, and a peak storage capacity of 5.98×10^8 m^3. The lake's primary economic value is as a fishery, but it is also important for agricultural and recreational uses. Like many other lakes in China, Lake Chagan is eutrophic, with high Chl-a content, and low Secchi disk transparency (SDT) (Duan et al. 2008): Chl-a is between 6.40 and 58.21 μg/L and SDT rarely exceeds 0.50 m (see Table 1). Since the Songhua River flows into Lake Chagan through a canal, it is the main water source for Lake Chagan. Water is also supplied to the lake by the Holin, Tao'er River, and Nenjiang Rivers, natural precipitation, and ground water.

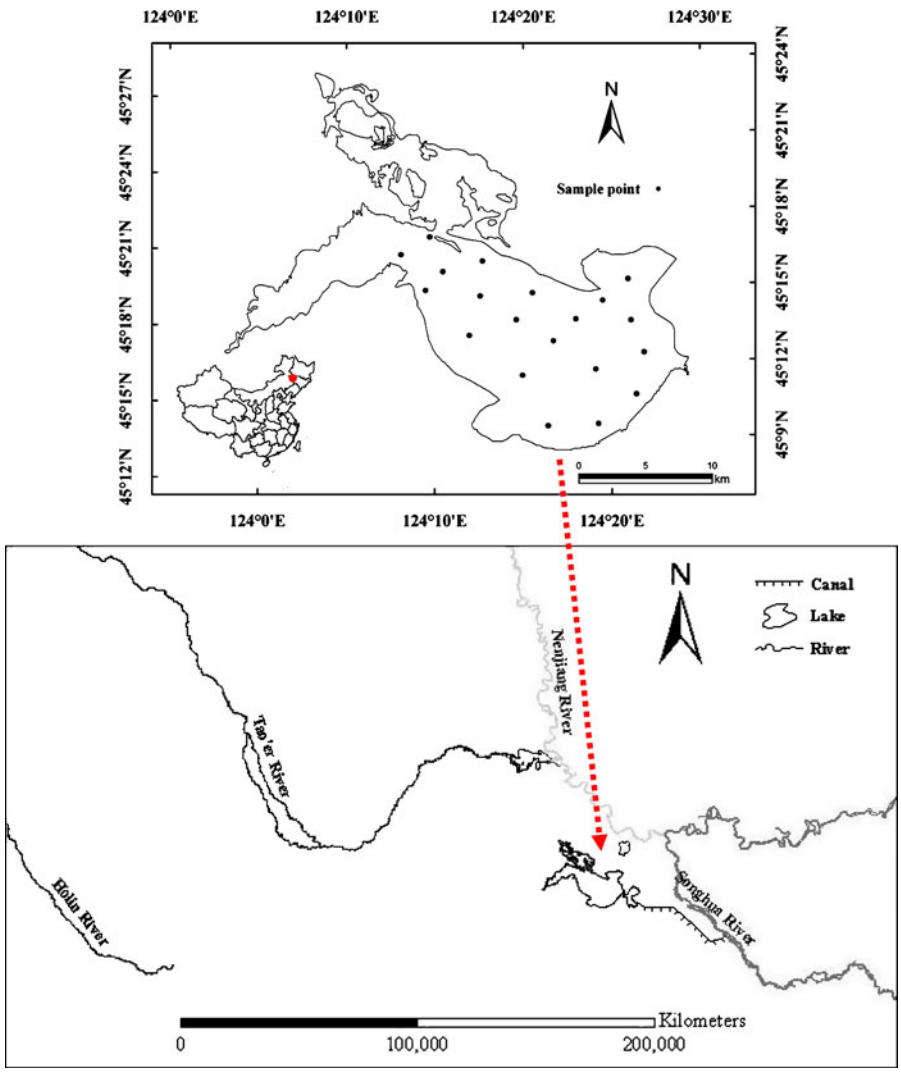

Fig. 1 Location of Lake Chagan in China

Table 1 Sample number and Chl-a concentration and secchi disk transparency in different months

Number	June 6	July 8	August 9	September 20	Summer 43
Chl-a ($\mu g \cdot L^{-1}$)					
Min	6.40	28.14	15.15	11.24	6.40
Max	14.68	58.21	37.15	47.23	58.21
Mean	10.22	40.57	28.81	24.38	26.34
SDT (m)					
Min	0.10	0.22	0.22	0.18	0.10
Max	0.46	0.24	0.30	0.32	0.46
Mean	0.25	0.23	0.25	0.25	0.25

Methodology

Water sampling and field spectral measurements

Water sampling and field spectral measurements were performed during the summer season from June to September in 2004. Due to the availability of water sample analysis in the laboratory, the number of water samples in different months varied from 6 to 20 for Lake Chagan (Table 1). In each fieldwork trip, the position of the sampling boat was geo-located by a portable Ashtech ProMark2 global position system receiver with

0.3–3 m accuracy specification. SDT and field spectral data were simultaneously measured at selected points in the lake. At each sampling site, the lake water was also collected with a clean bottle for further laboratory analysis within 4 h. A water sample was filtered using a glass micro-fiber filter (0.45 μm) to measure Chl-a with the standard spectro-photometric method. Acetone was used to extract Chl-a from the water sample for over 24 h. The sample was then read before and after its acidification using a spectro-photofluorometer. Finally, Chl-a was calculated by comparison with the known standards.

Field spectra were measured with a portable Fieldspec FSR VNIR® spectrometer (ASD Inc.). The ASD radiometer has a spectral range between 350 and 1,100 nm and a radiometric resolution of about 3 nm. Prior to the field campaign, the absolute radiance calibrations to the detector were performed. The measurements were taken from a boat platform above the lake surface, and the spectra were measured at least ten times at each sample station. A mean was taken as the final result. Each measured position was oriented to the boat side within the light propagation to minimize sun-glint from waves, but far away from the effect of the boat shadow.

Regression analysis

An alternative approach to the development of semi-empirical water color algorithms is by linear regression analysis. Linear regression fits an observed dependent data set (e.g., Chl-a concentration) using a linear combination of independent variables (e.g., reflectance values at discrete wavelengths). This leads to an algorithm based on regression analysis results, with the form as shown in Eq. 1:

$$C_{\text{chl-a}} = a + bx \tag{1}$$

where $C_{\text{chl-a}}$ is Chl-a concentration (μg/L), a and b are the regression coefficients, and x is the reflectance ratio or derivative reflectance at a specific wavelength (Wernand et al. 1998).

Results

Spectral characteristics of Chl-a

Chl-a is a phytopigment present in all algae groups in inland waters. Figure 2 shows reflectance spectra for the eutrophic Lake Chagan. It is common for inland water bodies of different trophic states. The resultant spectrum reveals a low reflectance value at wavelengths less than 500 nm, a phenomenon due to absorption by both algal pigments (e.g., Chl-a) and dissolved organic matter (Gitelson et al. 1993). Because of suspended matter influence, the absorption peak of the phytopigments Chl-a at 440 nm is not obviously visible. There is an increase in reflectance at wavelengths 510–620 nm, the result of low absorption by phytoplankton pigments coupled with an increase in backscattering when particle concentration increases. There are also two minima near 620 and 670 nm. These correspond to the absorption

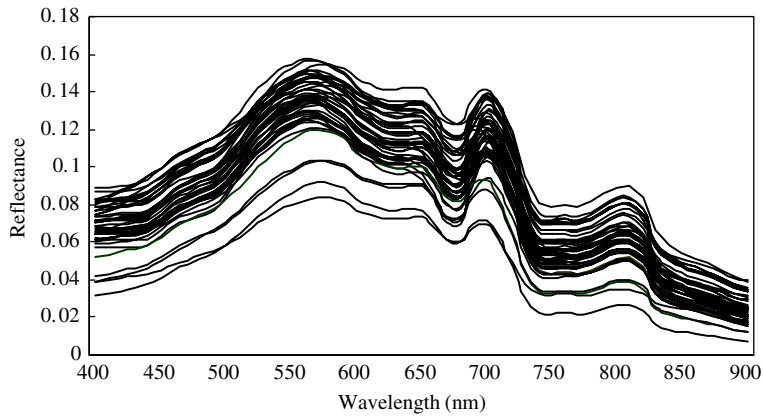

Fig. 2 Reflectance spectra over Lake Chagan

maxima of phytoplankton pigments (Gitelson 1992). Low reflectance at 620 nm is expected, due to absorption by cyanobacteria (e.g. phycocyanin; Schalles et al. 1998). At 670 nm, a reflectance minimum corresponds to the Chl-a absorption band. A peak of reflectance is also notable at 685–715 nm, due to fluorescence by Chl-a pigments (Gordon 1979). It reaches 700 nm for the increase of Chl-a contents in Lake Chagan.

First derivative

Derivative spectra indicate the rate of change of reflectance with wavelength ($dR(\lambda)/d\lambda$), which is the slope of the reflectance curve at wavelength λ (Han 2005). Derivative analysis enables the shape of the reflectance pattern to be correlated to chlorophyll concentrations. Figure 3a shows the first derivative reflectance curves for Lake Chagan. Note that the much greater variations among the spectral curves that appeared in Fig. 2 did not appear this time for their derivative spectra. This phenomenon indicated that derivative spectra were less affected by the wave effects and able to remove pure water effects. To test if the first derivative reflectance value at a specific wavelength can be used to estimate chlorophyll concentration, correlation coefficients were calculated for all bands. Figure 3b shows the results of correlation analysis performed on the first derivative and chlorophyll-a concentration; the first derivative had a much higher correlation with chlorophyll-a concentration. The higher correlation coefficients ($|R| > 0.8$) were found primarily in the spectral regions between 660 and 700 nm. These can be potential wavelength regions where the first derivative may be used to estimate chlorophyll-a concentration. It was found that with two-thirds of the samples ($n = 28$), the first derivative at 680 nm produced the highest positive correlation with chlorophyll-a concentration ($R^2 = 0.74$; Fig. 3c). In addition, one-third of the samples ($n = 15$) were chosen as test data to predict Chl-a concentration for their ability. As expected, the results were promising with a lower RMSE of 5.51 μg/L (Fig. 3d).

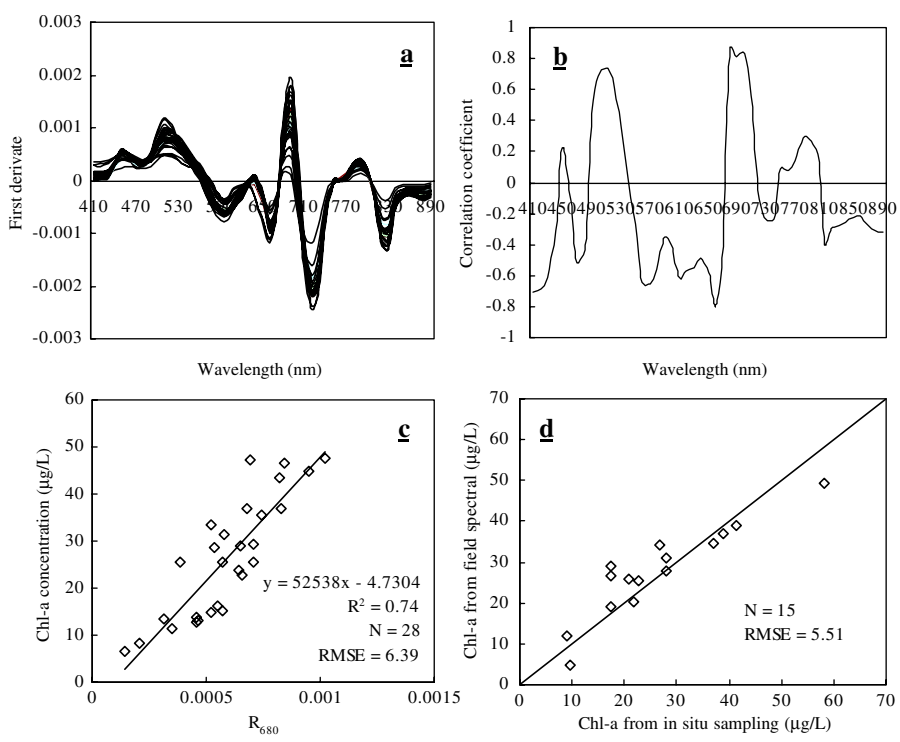

Fig. 3 First derivative: **a** first derivative spectra, **b** correlation coefficients (R), **c** regression model, **d** validation

Two-band model

Water color algorithm has been approached by using two-band ratios model, which shows characteristic optical trends of chlorophyll, one corresponding to high absorption and the other to low absorption. The advantage of using ratios over absolute values of reflectance is that they correct some of the effects of measurements geometrically and atmospherically (Koponen et al. 2001; Pulliainen et al. 2001). Previous studies have used statistical methods to link reflectance at certain wavelengths to changes in Chl-a concentration. In water color remote sensing, the four characteristic bands related to chlorophyll are the blue, green, red, and near infra-red (NIR) bands (Dekker et al. 1991; Mittenzwey et al. 1992; Han et al. 1994; Han and Rundquist 1997). In particular, wavelengths close to the 680 and 706 nm were found to be correlated with Chl-a concentration in most studies, which can enlarge their differences between the absorption maximum and the reflectance peak of Chl-a.

This study demonstrates that increases in Chl-a concentration have a consistent influence on the overall shape of the peak around 700 nm. Table 2 presents our analyses with wavelength positions in the absorption maximum and reflectance peak. These produced very similar relationships to those previously reported (Gitelson et al. 1993; Arenz et al. 1996), and $R_{710/670}$ is the optimal combination for accurately estimating Chl-a in the lake (see Fig. 4a). However, the absorption maximum and reflectance peak positions have a small shift in our datasets. Figure 4b shows regression model validation as derived from field spectra and Chl-a in situ measurements. It produced a larger R^2 of 0.84 with lower RMSE of 5.38 μg/L. The results from these empirical studies support the current hypothesis that spectral absorptions and reflectance near the red and infrared bands represent a sound physical basis for estimating Chl-a concentration.

Three-band model

Recently, a conceptual three-band model was developed for estimating Chl-a amounts (Gitelson et al. 2003) and had been confirmed its robust use in turbid, productive waters (Dall'Olmo and Gitelson 2006). Based on the expression of remote sensing reflectance as follows, the model is devised to isolate Chl-a absorption coefficient from reflectance spectra (Gitelson et al. 2008):

$$\left[R_{rs}^{-1}(\lambda_1) - R_{rs}^{-1}(\lambda_2)\right] \times R_{rs}(\lambda_3) \quad (2)$$

where $R_{rs}(\lambda_i)$ was reflectance in band λ_i. When λ_i falls in the region where $R_{rs}(\lambda_i)$ is maximally sensitive to the phytoplankton pigments absorption (a_{ph}), and λ_2 falls in the region where $R_{rs}(\lambda_2)$ is minimally sensitive to a_{ph}($a_{ph}(\lambda_2) << a_{ph}(\lambda_1)$) and absorption by other constituents at λ_2 is almost equal to that at λ_1. Therefore, the effects of backscattering (b_b) by all particulate matters are expected to be minimized by the third band λ_3. Since that, λ_1 must be ranged between 660 and 690 nm (Dall'Olmo and Gitelson 2006), and λ_2 should be in the range from 670 to 710 nm, while λ_3 beyond 710 nm (Xu et al. 2009).

In order to optimize the three band positions, an iteration algorithm was developed using

Table 2 Regressive equations and relation coefficients indicating the relationship between Chl-a content and spectral reflectance ratios in Lake Chagan

Band ratio	Regressive equation	R^2	Band ratio	Regressive equation	R^2
710/440	$Y = 55.792x - 58.548$	0.31	710/670	$y = 83.328x - 69.277$	0.70
700/670	$Y = 96.469x - 91.893$	0.69	710/680	$y = 79.192x - 66.653$	0.67
810/670	$Y = 87.941x - 30.721$	0.55	750/680	$y = 91.28x - 25.916$	0.51
560/440	$Y = 15.3x - 2.6142$	0.05	750/580	$y = 78.296x - 4.8761$	0.16
710/660	$Y = 109.03x - 85.96$	0.67	700/680	$y = 90.278x - 86.889$	0.65
700/690	$Y = 208.24x - 199.19$	0.65	700/660	$y = 140.87x - 128.67$	0.69
710/690	$y = 143.33x - 118.89$	0.63	710/580	$y = 122.84x - 73.895$	0.29

x means the band ratio, y refers to Chl-a

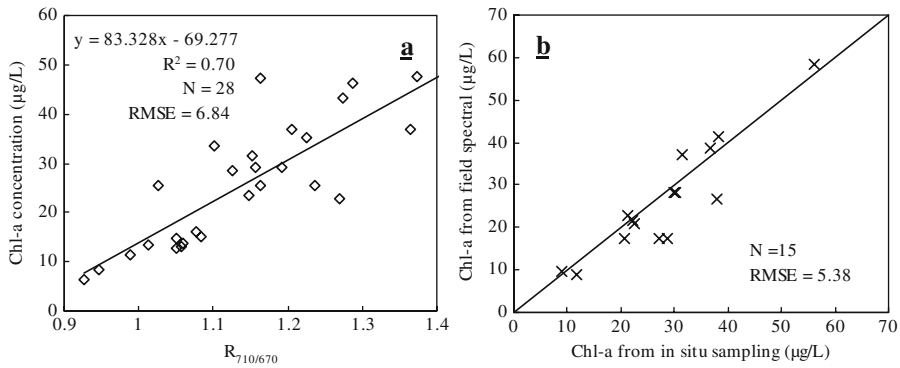

Fig. 4 Regression equation derived from $R_{710/670}$ and validation: **a** regression model, **b** validation

Matlab software. To find the optimal λ_1, the initial positions for λ_2 within 670 to 710 nm and λ_3 beyond 710 nm were set. As λ_1 was tuned from 660 to 690 nm, the correlation coefficient of $[R_{rs}^{-1}(\lambda_1) - R_{rs}^{-1}(\lambda_2)] \times R_{rs}(\lambda_3)$ with Chl-a was calculated. Its maximum occurs at 670 nm, which was selected for λ_1. Then in the tuning of λ_2, 690 nm was phased in as the optimal position. When proper positions for λ_1, λ_2 were fixed, the three-band model showed a well correlation with Chl-a while $\lambda_3 = 740$ nm in the whole tuning range. Thus, the final optimal positions for λ_1, λ_2, and λ_3 were 670, 690, and 740 nm, respectively. Figure 5a shows the linear regression equation with $R^2 = 0.72$, and RMSE = 6.58 μg/L. In order to be useful for remote sensing, an algorithm for predicting Chl-a concentration should be applicable and regression equations should be tested for their ability to predict Chl-a concentration for new data sets. By using the independent date set ($n = 15$), the regression equations were then used to predict the Chl-a concentrations, and the results were summarized in Fig. 5b.

Reverse continuum removal method

Except traditional semi-algorithms, a new approach named reverse continuum removal was developed to isolate the peak around 700 nm which has showed a sensitive correlation with Chl-a in previous reports (Gitelson 1992; Gower and Borstad 2004). Continuum removal is a method commonly used in laboratory infrared spectroscopy (Ingle and Crouch 1998). The continuum is a convex hull fitted over the top of a spectrum utilizing straight line segments that connect local spectra maxima. The continuum is removed by dividing the reflectance value for each point in the absorption pit by the reflectance level of the continuum line (convex hull) at the corresponding wavelength (Mutanga et al. 2003). The first and last spectral data values are on the hull and therefore the first and last bands in the output continuum-removed data file are equal to 1. The output curves have values between 0 and 1, in which the absorption pits are enhanced and the absolute variance is removed (Schmidt and

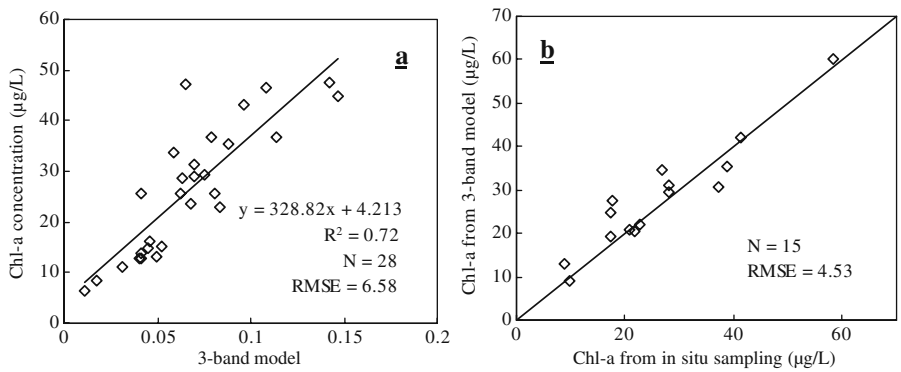

Fig. 5 Three-band model: **a** regression model, **b** validation

Skidmore 2001). Continuum-removed absorption features can be compared by being scaled to the same depth at the band center, thus allowing a comparison of the shapes of absorption features.

Although continuum removal is easily used to isolate absorption features, it is difficult to retrieve reflectance peaks. However, if we use reverse continuum over the bottom of a spectrum with common line segments, the reflectance peak will be easily isolated and compared. To compare the shapes of the peak around 700 nm between samples, the initial step is to calculate the equation for a line between the continuum end points of the reflectance data (Fig. 6a). Next, the reflectance value for each point in the reflectance band is divided by the reflectance level of the continuum line at the corresponding wavelength to establish the continuum-removed spectral features (Fig. 6b and c). Band depths in each absorption feature are normalized. Normalization is investigated using the depth at the center of the feature and also the area under the band depth curve (Kokaly and Clark 1999). The area of each peak can be computed through mathematical integral theory, and the depth of each peak (D) is computed from the equation:

$$D = R_a / R_b - 1 \tag{3}$$

where R_a is the reflectance value at the centre of the peak, and R_b is the reflectance of the continuum at the same wavelength as R_a (see Fig. 6b and d).

Normalized peak depth and area with the reverse continuum-removed methods were analyzed using a regression routine in order to determine shape characters correlated with Chl-a (Fig. 7). The regression equation fits an observed dependent set that Chl-a using independent variables such as the peak depth and area. Regression models developed from the training data set were used to predict Chl-a concentration in an independent test data set. Linear regressions were firstly applied to the normalized peak depth and area of these data to establish regression equations. Figure 8a and b show the R^2 and root mean square error (RMSE) for shape features of the peak around 700 nm and Chl-a. Correlations were

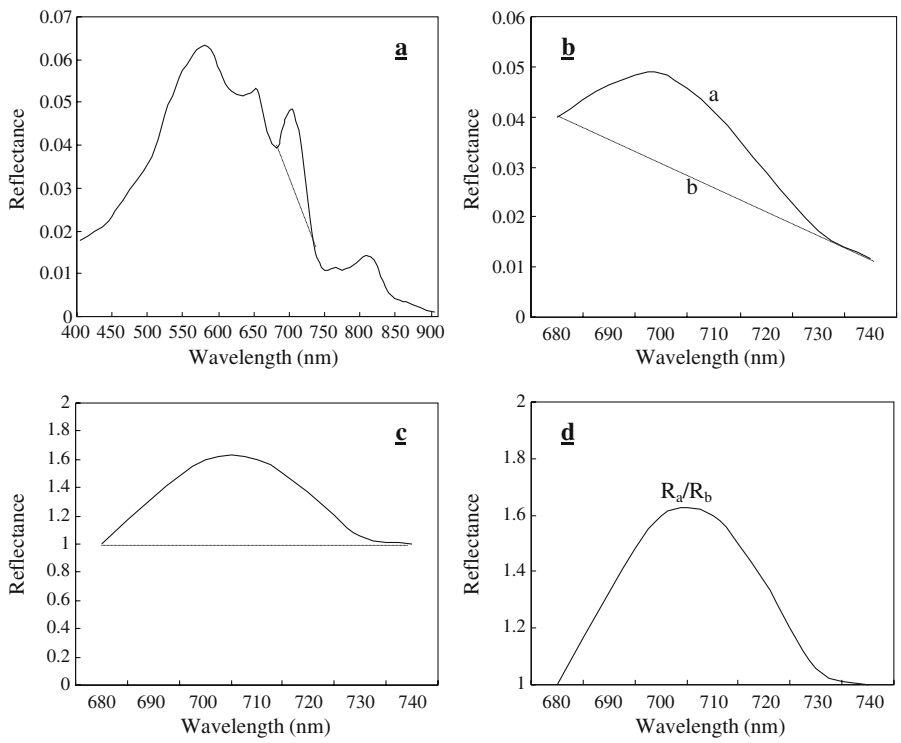

Fig. 6 A sketch map of reverse continuum removal for isolated the reflectance peak

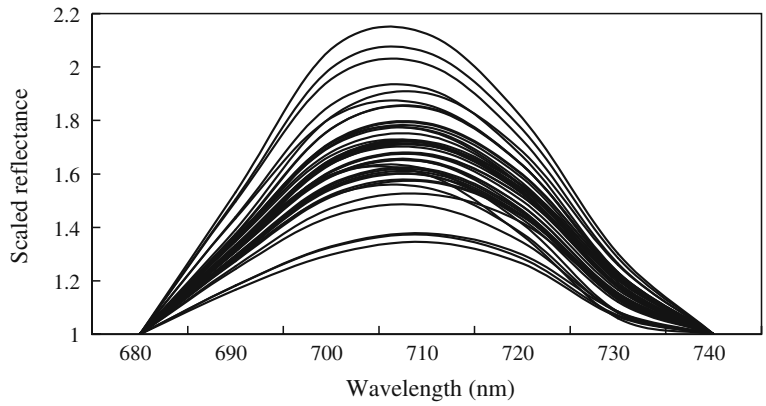

Fig. 7 Isolated peaks around 700 nm of all samples in Lake Chagan

high (R^2 from 0.65 to 0.67) and RMSE were low (RMSE from 7.36 μg/L to 7.22 μg/L), which reveal that peak area has a better correlation than peak depth:

$$C_{\text{Chl-a}} = 63.047\text{Depth} - 17.205 \quad (4)$$

$$C_{\text{Chl-a}} = 1.7305\text{Area} - 16.868 \quad (5)$$

The validation results are presented in Fig. 8c and d. As expected, correlations were highest and RMSE lowest for the predictions of the remaining samples. In general, they are both significantly related to Chl-a, which means they have a similar physical significance for Chl-a.

Application of algorithms to MERIS

The medium resolution imaging spectrometer (MERIS) onboard Envisat was successfully launched on 1 March, 2002 (Sørensen et al. 2007) has been designed mainly for ocean and coastal water remote sensing (Doerffer and Schiller

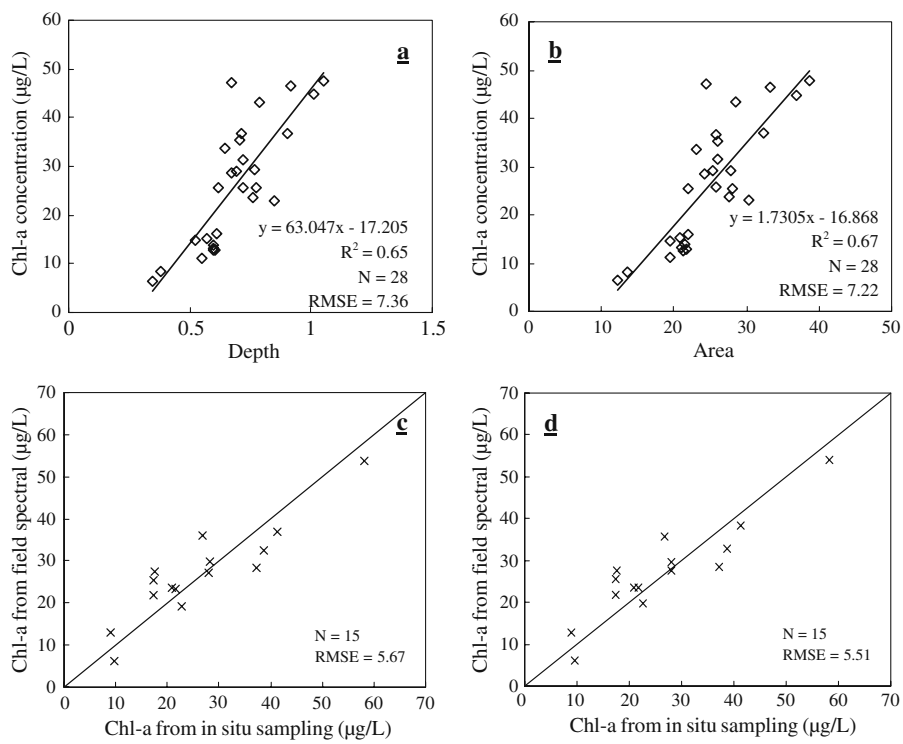

Fig. 8 Regression equation for Chl-a concentration applied to peak depth and area: **a** peak depth linear equations, **b** peak area linear equations, **c** peak depth validation, **d** peak area validation

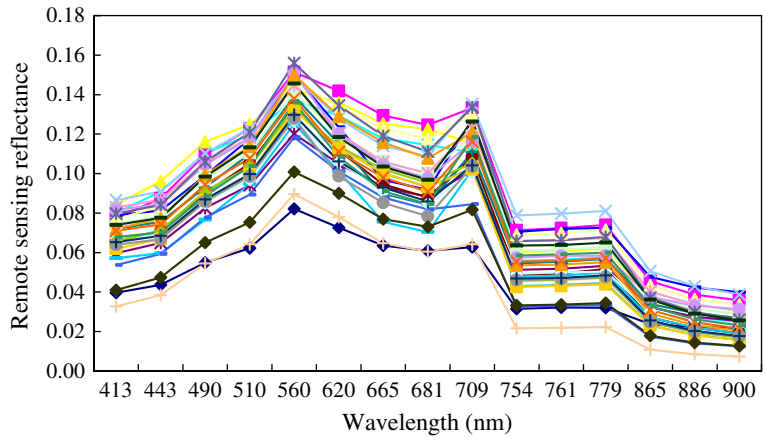

Fig. 9 MERIS-simulated reflectance spectra resampled with regard to their center wavelengths

2007). The features of MERIS designed for coastal water are the spatial resolution of 300 m together with a revisit period of 1 to 3 days (latitude dependent), 15 narrow spectral bands in the visible and near infrared wavelengths. With these features, MERIS is a suitable sensor and can be used for monitoring of at least larger inland waters, such as Lake Chagan. Therefore, it's necessary to determine the suitability of existing semi-empirical algorithms for MERIS.

Field spectra were resampled with regard to their center wavelengths applied to MERIS (Fig. 9). Apparently, the first derivative and reverse continuum removal algorithms are not suitable for MERIS, because they need continuous spectrum. Although MERIS owns 15 narrow bands within 400 and 900 nm, it's not enough to meet the requirement. The two-band model was calibrated with the spectral bands of MERIS ($\lambda_1 = 709$ nm, $\lambda_2 = 685$ nm). The relationship

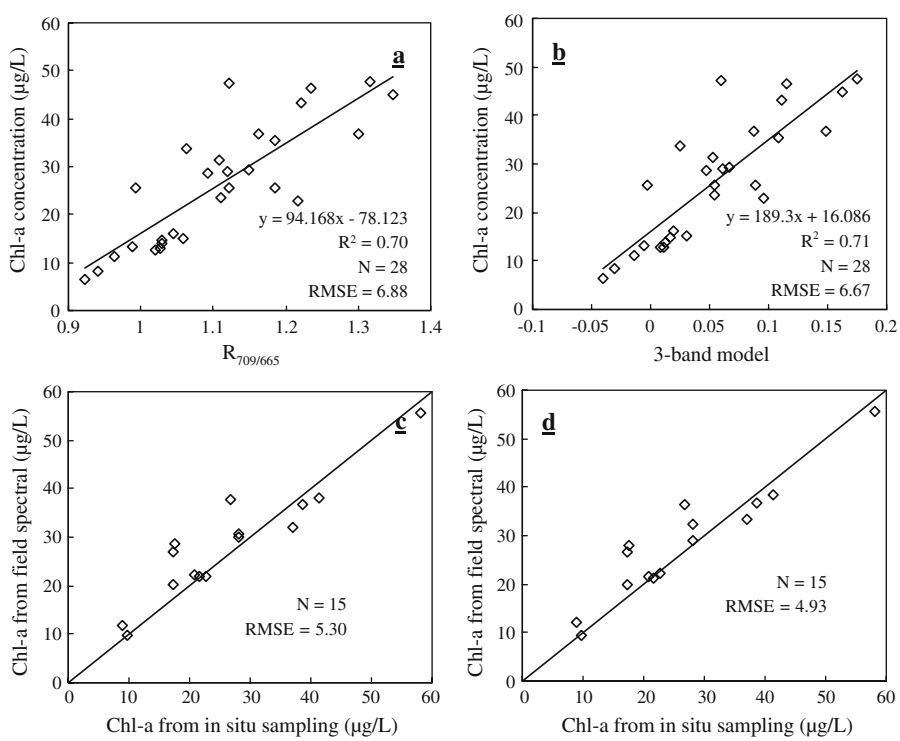

Fig. 10 Regression equation for Chl-a concentration applied to MERIS: **a** two-band model, **b** three-band model, **c** two-band model validation, **d** three-band model validation

between Chl-a concentration and the two-band model was also found to be linear and highly significant ($R^2 = 0.70$, Fig. 10a). We also evaluated the accuracy of the three-band algorithm with MERIS spectral bands (Eq. 2) for monitoring Chl-a concentrations in Lake Chagan. Importantly, the three-band algorithm was calibrated and validated with MERIS system ($\lambda_1 = 665, \lambda_2 = 709, \lambda_3 = 754$) has some shift compare to the channels of spectral bands ($\lambda_1 = 670, \lambda_2 = 690, \lambda_3 = 740$). Therefore, the errors of Chl-a prediction by the three-band algorithm for the simulated MERIS bands are a bit larger (RMSE = 6.67 μg/L, Fig. 10b) than that for field spectral (RMSE = 6.58 μg/L, Fig. 5a). Comparison of the measured and predicted estimates of Chl-a, both the two-band and the three-band models showed promising results with the independent data set ($n = 15$; Fig. 10c and d). In summary, the three-band algorithm could be used for accurate quantitative monitoring of Chl-a using field spectral and MERIS.

Discussion and conclusion

Lake Chagan is a typical Case II water system and a eutrophic to hypereutrophic lake by TSI standard criteria (Duan et al. 2008), where red and near infrared reflectances are consistently the most reliable and expedient remote sensing variables in predictive algorithms for Chl-a assessments (Schalles et al. 1998). Results show that the coefficient of variation of reflectance including the first derivative reflectance and two-band ratios in this region of the spectrum is maximal sensitivity of Chl-a concentration.

Some major findings reveal that the first-order derivative is able to remove pure water effects, and derivative spectra are an objective tool in isolating the absorption features of phytoplankton. Therefore, the first derivative corresponding to the absorption feature shows a good correlation with Chl-a. Han and Rundquist (1997) observed that the first derivative was correlated better with the chlorophyll than the NIR/red ratio, and the highest correlation between the first derivative and chlorophyll occurred at 690 nm. Fraser (1998) found that the first derivatives at 429 and 695 nm were correlated significantly with Chl-a concentration. In Lake Chagan, Chl-a absorbance at 670 nm was offset by the scattering behavior of algal cells and was a point of minimum sensitivity to algal concentration. The magnitude of the peak near 710 nm depends on scattering by all particles and is correlated with chlorophyll via the link between chlorophyll concentration and algal biomass (Gitelson 1992; Gitelson et al. 1995; Fraser 1998; Lee and Carder 2000; Dall'Olmo and Gitelson 2006). As algal biomass increases, both scattering and the resultant reflectance value increases. In this study, NIR/red ratio and first derivative reflectance are both effective predictors of algal–chlorophyll concentration. The first derivative of reflectance, on the other hand, is better correlated with chlorophyll concentration than the 710/670 band ratio. The highest correlation between the first derivative and chlorophyll was at 680 nm.

In semi-empirical algorithms, two-band ratios are popular and widely used, and remain sensitive over a wider dynamic range of absorption values and perform better at low- and high-absorption values (Lee and Carder 2000). Band ratios can also be used with satellite data such as Landsat and MERIS to reduce the topographic and atmospheric effects of remote sensing (Kokaly and Clark 1999). Apparently, the two-band ratios model is a special case of the three-band model developed recently when $a_{\text{chl-a}}(\lambda) \geq b_{\text{b}}$, and $a_{\text{chla}}(\lambda) \geq a_{\text{tripton}}(\lambda) + a_{\text{CDOM}}(\lambda)$. However, some of the water bodies studied might not hold for the key assumptions (Gitelson et al. 2008), the three-band model in Lake Chagan show a higher resolution.

Compared with the models using the first derivative at 680 nm and the two-band ratios and three-band algorithms, reverse continuum removal analysis did not fare noticeably better than other analytical approaches. However, this new approach can be used easily to isolate the peak features. Because of the variability in the Chl-a specific absorption coefficient and other factors in different water bodies, it will affect the accuracy of Chl-a estimation considerably (Dall'Olmo and Gitelson 2006). Therefore, the optimal bands of the NIR/red ratio and the first derivative have to

be adjusted and selected again. This avoids the need to set fresh parameters for the models for water bodies with specific optical properties, as the peak around 700 nm is apparent and can easily be picked out in order to minimize these effects. Once the spectral configuration is determined and understood, it is possible to specify a simple model with sufficient sensitivity to measure accurately the Chl-a concentration.

Previous studies have showed that the peak height, which was quantified by measuring the difference between reflectance at the wavelength, where the maximum reflectance is observed and the baseline interpolated from measurements in the peak around 700 nm, correlated well with the Chl-a concentration (Gitelson 1992). Compared with peak height, peak depth used in reverse continuum removal is not the difference but the ratio between different reflectances. Peak height is always calculated from the original data (Gitelson 1992), but peak depth is calculated from the data after normalization using reverse continuum removal analysis (Figs. 2 and 3). In general, results indicate that they are both significantly related to Chl-a, which means they have a similar physical significance for Chl-a.

The peak around 700 nm is important for the remote sensing of inland and coastal waters with regard to measuring chlorophyll. Therefore, the corresponding region seems more appropriate for retrieval information on phytoplankton concentration from reflectance spectra. The magnitude of the peak near 700 nm depends on scattering by all particles and is correlated with chlorophyll via the link between Chl-a concentration and the reflectance changes including peak depth and area. The normalization approach in the predictive models is effective because the slope of the reference baseline fitted between 680 and 740 nm and its magnitude above zero reflectance depend primarily on scattering by nonalgal seston (Schalles et al. 1998). With variation of organic and nonpigmented inorganic suspended matter, the baseline changes but has minimal influence on the depth and area of the peak above this baseline. Thus, reflectance depth and area above the baseline depends almost entirely on phytoplankton density and is a useful measure of Chl-a (Gitelson 1992; Gitelson et al. 1995; Fraser 1998).

All of the algorithms mentioned show a better correlation and can be used to predict Chl-a concentration. Because the number of sampling points is different in each month, it may produce some errors to the algorithms. Water quality variables are continually changing over time. Therefore, a different number of sampling points may not lead to a comprehensive representative of water quality during each month. When the sampling points are limited, the algorithms may be affected and their precision will be reduced. Fortunately, the 4 months from June to September all fall within the summer season, with the result that water quality variables such as Chl-a and SDT (See Table 1) in Lake Chagan do not differ significantly. This helps limit and control the possible errors in the algorithms.

Acknowledgements We would like to acknowledge the financial supports provided by the National Natural Science Foundation of China (No.40801137, No.40871168, and No.40671138), the Special Prize of President Scholarship for Postgraduate Students of the Chinese Academy of Sciences (No.07YJ011001), and the Knowledge Innovation Program of the Chinese Academy of Sciences (No.CXNIGLAS200807). Thanks also for two anonymous reviewers for their critical comments.

References

Arenz, R. F., Lewis, W. M., & Saunders, J. F. (1996). Determination of chlorophyll and dissolved organic carbon from reflectance data for Colorado reservoirs. *International Journal of Remote Sensing, 17*, 1547–1566. doi:10.1080/01431169608948723.

Dall'Olmo, G., & Gitelson, A. A. (2006). Effect of bio-optical parameter variability and uncertainties in reflectance measurements on the remote estimation of chlorophyll-a concentration in turbid productive waters: Modeling results. *Apply Optics, 45*, 3577–3592. doi:10.1364/AO.45.003577.

Dekker, A. G., Malthus, T. J., & Seyhan, E. (1991). Quantitative modeling of inland water quality for high resolution MSS systems. *IEEE Transaction on Geoscience and Remote Sensing, 29*, 89–95. doi:10.1109/36.103296.

Doerffer, R., & Schiller, H. (2007). The MERIS Case 2 water algorithm. *International Journal of Remote Sensing, 28*, 517–535. doi:10.1080/01431160600821127.

Duan, H., Zhang, Y., Zhang, B., Song, K., Wang, Z., Liu, D., et al. (2008). Estimation of chlorophyll-a concentration and trophic states for inland lakes in Northeast China from Landsat TM data and field spectral measurements. *International Journal of Remote Sensing, 29*, 767–786. doi:10.1080/01431160701355249.

Feng, H., Campbell, J. W., Dowell, M. D., & Moore, T. S. (2005). Modeling spectral reflectance of optically complex waters using bio-optical measurements from Tokyo Bay. *Remote Sensing of Environment, 99*, 232–243. doi:10.1016/j.rse.2005.08.015.

Fraser, R. N. (1998). Hyperspectral remote sensing of turbidity and chlorophyll a among Nebraska Sand Hills lakes. *International Journal of Remote Sensing, 19*, 1579–1589. doi:10.1080/014311698215360.

Giardino, C., Pepe, M., Brivio, P. A., Ghezzi, P., & Zilioli, E. (2001). Detecting chlorophyll, Secchi disk depth and surface temperature in a sub-alpine lake using Landsat imagery. *The Science of the Total Environment, 268*, 19–29. doi:10.1016/S0048-9697(00)00692-6.

Gitelson, A. (1992). The peak near 700 nm on radiance spectra of algae and water: Relationship of its magnitude and position with chlorophyll concentration. *International Journal of Remote Sensing, 13*, 3367–3373. doi:10.1080/01431169208904125.

Gitelson, A., Garbuzov, G., Szilagyi, F., Mittenzwey, K.-H., & Karnieli, A. (1993). Quantitative remote sensing methods for real-time monitoring of inland waters quality. *International Journal of Remote Sensing, 14*, 1269–1295. doi:10.1080/01431169308953956.

Gitelson, A., Laorawat, S., Keydan, G., & Vonshak, A. (1995). Optical properties of dense algal cultures outdoors and its application to remote estimation of biomass and pigment concentration in Spirulina platensis. *Journal of Phycology, 31*, 828–834. doi:10.1111/j.0022-3646.1995.00828.x.

Gitelson, A. A., Dall'Olmo, G., Moses, W., Rundquist, D. C., Barrow, T., Fisher, T. R., et al. (2008). A simple semi-analytical model for remote estimation of chlorophyll-a in turbid waters: Validation. *Remote Sensing of Environment, 112*, 3582–3593. doi:10.1016/j.rse.2008.04.015.

Gitelson, A. A., Gritz, Y., & Merzlyak, M. N. (2003). Relationship between leaf chlorophyll content and spectral reflectance and algorithms for nondestructive chlorophyll assessment in higher plant leaves. *Journal of Plant Physiology, 160*, 271–282. doi:10.1078/0176-1617-00887.

Gordon, H. (1979). Diffusive reflectance of the ocean: The theory of its augmentation by chlorophyll-2a fluorescence at 685 nm. *Applied Optics, 18*, 1161–1166.

Gower, J. F. R., & Borstad, G. A. (2004). On the potential of MODIS and MERIS for imaging chlorophyll fluorescence from space. *International Journal of Remote Sensing, 25*, 1459–1464. doi:10.1080/01431160310001592445.

Han, L. (2005). Estimating chlorophyll-a concentration using first-derivative spectra in coastal water. *International Journal of Remote Sensing, 26*, 5235–5244. doi:10.1080/01431160500219133.

Han, L., & Rundquist, D. C. (1997). Comparison of NIR/RED ratio and first derivative of reflectance in estimating algal-chlorophyll concentration: A case study in a turbid reservoir. *Remote Sensing of Environment, 62*, 253–261. doi:10.1016/S0034-4257(97)00106-5.

Han, L., Rundquist, D. C., Liu, L. L., & Fraser, L. N. (1994). The spectral responses of algal chlorophyll in water with varying levels of suspended sediment. *International Journal of Remote Sensing, 15*, 3707–3718. doi:10.1080/01431169408954353.

Ingle, J. D., & Crouch, S. R. (1998). *Spectrochemical analysis*. Englewood Cliffs, New Jersey: Prentice Hall.

Kokaly, R. F. (2001). Investigating a physical basis for spectroscopic estimates of leaf nitrogen concentration. *Remote Sensing of Environment, 75*, 153–161. doi:10.1016/S0034-4257(00)00163-2.

Kokaly, R. F., & Clark, R. N. (1999). Spectroscopic determination of leaf biochemistry using band-depth analysis of absorption features and stepwise multiple linear regression. *Remote Sensing of Environment, 67*, 267–287. doi:10.1016/S0034-4257(98)00084-4.

Koponen, S., Pulliainen, J., Kallio, K., & Hallikainen, M. (2002). Lake water quality classification with airborne hyperspectral spectrometer and simulated MERIS data. *Remote Sensing of Environment, 79*, 51–59. doi:10.1016/S0034-4257(01)00238-3.

Koponen, S., Pulliainen, J., Servomaa, H., Zhang, Y., Hallikainen, M., Kallio, K., et al. (2001). Analysis on the feasibility of multisource remote sensing observations for Chl-a monitoring in Finish lakes. *The Science of the Total Environment, 268*, 95–106. doi:10.1016/S0048-9697(00)00689-6.

Kutser, T., Herlevi, A., Kallio, K., & Arst, H. (2001). A hyperspectral model for interpretation of passive optical remote sensing data from turbid lakes. *The Science of the Total Environment, 268*, 47–58. doi:10.1016/S0048-9697(00)00682-3.

Lee, Z. P., & Carder, K. L. (2000). Band-ratio or spectral-curvature algorithms for satellite remote sensing. *Applied Optics, 39*, 4377–4380. doi:10.1364/AO.39.004377.

Mittenzwey, K. H., Gitelson, A., Ullrich, S., & Kondratyev, K. Y. (1992). Determination of chlorophyll a of inland waters on the basis of spectral reflectance. *Limnology and Oceanography, 37*, 147–149.

Mutanga, O., Skidmore, A. K., & Van Wieren, S. (2003). Discriminating tropical grass (Cenchrus ciliaris) canopies grown under different nitrogen treatments using spectroradiometry. *ISPRS Journal of Photogrammetry and Remote Sensing, 57*, 263–272. doi:10.1016/S0924-2716(02)00158-2.

Pulliainen, J., Kallio, K., Eloheimo, K., Koponen, S., Servomaa, H., Hannonen, T., et al. (2001). A semi-operative approach to lake water quality retrieval from remote sensing data. *The Science of the Total Environment, 268*, 79–93. doi:10.1016/S0048-9697(00)00687-2.

Richardson, L. (1996). Remote sensing of algal bloom dynamics. *BioScience, 46*, 492–501.

Ritchie, J. C., Cooper, C. M., & Schiebe, F. R. (1990). The relationship of MSS and TM digital data with suspended sediments, chlorophyll, and temperature in Moon Lake, Mississippi. *Remote Sensing of Environment, 33*, 137–148. doi:10.1016/0034-4257(90)90039-O.

Schalles, J. F., Gitelson, A., Yacobi, Y. Z., & Kroenke, A. E. (1998). Estimation of chlorophyll from time

series measurements of high spectral resolution reflectance in an eutrophic lake. *Journal of Phycology, 34*, 383–390. doi:10.1046/j.1529-8817.1998.340383.x.

Schmidt, K. S., & Skidmore, A. K. (2001). Exploring spectral discrimination of grass species in African rangelands. *International Journal of Remote Sensing, 22*, 3421–3434. doi:10.1080/01431160152609245.

Sørensen, K., Aas, E., & Høkedal, J. (2007). Validation of MERIS water products and bio-optical relationships in the Skagerrak. *International Journal of Remote Sensing, 28*, 555–568. doi:10.1080/01431160600815566.

Wernand, M. R., Shimwell, S. J., Boxall, S., & Van Aken, H. M. (1998). Evaluation of specific semi-empirical coastal colour algorithms using historic data sets. *Aquatic Ecology, 32*, 73–91. doi:10.1023/A:1009946501534.

Xu, J. P., Li, F., Zhang, B., Song, K. S., Wang, Z. M., Liu, D. W., et al. (2009). Estimation of chlorophyll-a concentration using field spectral data: A case study in inland Case-II waters, North China. *Environmental Monitoring and Assessment*. doi:10.1007/s10661-008-0568-z.

Zhang, Y., Koponen, S., Pulliainen, J., & Hallikainen, M. (2002). Application of an empirical neural network to surface water quality estimation in the Gulf of Finland using combined optical data and microwave data. *Remote Sensing of Environment, 81*, 327–336. doi:10.1016/S0034-4257(02)00009-3.